Reactions of DNA Purines with Dirhodium Formamidinate Compounds That Display Antitumor Behavior

K. V. Catalan, J. S. Hess, M. M. Maloney, D. J. Mindiola, D. L. Ward, and K. R. Dunbar*,†

Department of Chemistry, Michigan State University, East Lansing, Michigan 48824

Received February 17, 1999

The synthesis and characterization of products from reactions of $Rh_2(form)_2(O_2CCF_3)_2(CH_3CN)_2$ (form = N,N'-p-ditolylformamidinate, N,N'-diphenylformamidinate) and the partially solvated $[Rh_2(DTolF)_2(CH_3CN)_6][BF_4]_2$ (DtolF = N,N'-p-ditolylformamidinate) with the DNA purine analogues, 9-ethylguanine, and 9-ethyladenine are described. X-ray crystallography was used to characterize $Rh_2(DTolF)_2(O_2CCF_3)_2(CH_3CN)_2$ (**1**) which crystallizes in the space group $P2_1/n$ with a = 10.849 (3) Å, b = 21.435 (6) Å, c = 18.677 (3) Å, V = 4340 Å³, Z = 4, R = 0.0451, and R_w = 0.0904. The two rhodium centers are bridged by four $O_2CCF_3^-$ ligands with a Rh−Rh distance of 2.24743(5) Å. Compound **1** reacts with 9-ethylguanine to form $Rh_2(DTolF)_2(9\text{-EtGH})_2(O_2CCF_3)_2$ (**3**) which exists as two isomers, namely head-to-head and head-to-tail as confirmed by ¹H NMR spectroscopy. $[Rh_2(DTolF)_2(CH_3CN)_6][BF_4]_2$ (**5**) crystallizes in the *Pbca* space group with a = 21.646 (3) Å, b = 31.272 (3) Å, c = 14.561(4) Å, V = 9857 Å³, Z = 8, R = 0.046, and R_w = 0.063. The Rh−Rh bond distance is 2.5594 (8) Å. The partially solvated compound **5** reacts with 9-ethyladenine and 9-ethylguanine to form $[Rh_2(DTolF)_2(9\text{-EtAH})_2(CH_3CN)][BF_4]_2$ (**6**) and $[Rh_2(DTolF)_2(9\text{-EtGH})_2(CH_3CN)][BF_4]_2$ (**7**), respectively. Compound **6** was characterized by X-ray crystallography as well as by variable temperature ¹H NMR spectroscopy. $[Rh_2(DTolF)_2$-$(9\text{-EtAH})_2(CH_3CN)][BF_4]_2$ crystallizes in the $P2_1/c$ space group with a = 15.648(8) Å, b = 16.575(5) Å, c = 20.026(8) Å, β = 105.17(4)°, V = 4994 Å³, Z = 4, R = 0.063, and R_w = 0.073. This compound contains two bridging DTolF⁻ ligands as well as two 9-ethyladenine ligands bridging through the N7 and exocyclic N6 positions in a head-to-tail fashion. ¹H NMR studies performed on **6** revealed that the N6 position is in the imino (NH⁻) form.

Introduction

Since the recognition that cisplatin (Figure 1a) is an effective antitumor agent, researchers have discovered many additional examples of biologically active transition metal compounds.[1a] Among these are the dirhodium tetracarboxylate complexes $Rh_2(O_2CR)_4L_2$ (R = Me, Et, Ph, or CF_3; L = donor solvent) that are active against such tumors as human oral carcinoma, Ehrlich ascites, L1210, and P388 (Figure 1b).[1]

Twenty years have passed since the first biological studies were performed on dirhodium compounds, yet little is known about the potential mechanism of their antitumor activity. The main conclusions that one can glean from the literature is that the compounds inhibit DNA synthesis in a manner akin to cisplatin and that they exhibit a strong preference for binding to adenine over guanine.[2,3] The affinity for axially bound adenine
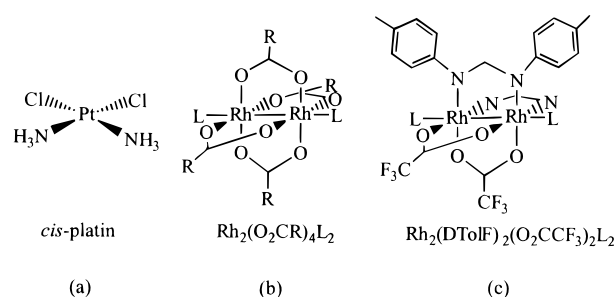

Figure 1. Transition metal antitumor compounds (a) cis-platin, (b) dirhodium tetracarboxylate, and (c) dirhodium formamidinate/carboxylate.

is easily understood by an examination of the X-ray structure of the bis(1-methyladenosine) adduct of $Rh_2(OAc)_4$, which exhibits hydrogen bonding between the exocyclic amine groups and the bridging carboxylate oxygen atoms.[2e] Since most reactions of these compounds occur at the axial positions, the argument was advanced that guanine bases would be precluded from reacting with dirhodium tetracarboxylates due to repulsive interactions between the ketone oxygen and the carboxylate bridges.[3] While this may pose a problem for *axial* binding of guanine, it does not preclude binding through the equatorial sites and, indeed, $Rh_2(OAc)_4$ and numerous related compounds are quite reactive toward guanine. X-ray data revealed that the purine ligands are not bound axially, as previously noted for adenine-type bases, but rather equatorially via bridging interactions involving the N7 and ketone O6 positions (Figure 2).[4]

---

* To whom correspondence should be addressed. E-mail: dunbar@mail.chem.tamu.edu.

† Present address: Texas A&M University.

(1) (a) Rosenberg, B.; Van Camp, L. *Nature* **1969**, *222*, 385. (b) Pruchnik, F.; Dus, D. *J. Inorg. Biochem.* **1996**, *61*, 55. (c) Bear, J. L.; Gray, H. B.; et al. *Cancer Chemother. Rep.* **1975**, *59*, 611. (d) Bear, J. L.; Howard, R. A.; Dennis, A. M. *Curr. Chemother., Proc. Int. Congr. Chemother., 10th* **1977**, *2*.

(2) (a) Pneumatikakis, G.; Hadjiliadis, N. *J. Chem. Soc., Dalton Trans.* **1979**, 596. (b) Rainen, L.; Howard, R. A.; Kimball, A. P.; Bear, J. L. *J. Inorg. Chem.* **1975**, *11*, 2752. (c) Farrell, N. *J. Inorg. Biochem.* **1981**, *14*, 261. (d) Yu, B. S.; Choo, S. Y. *J. Pharm. Soc. Kor.* **1975**, *19*, 215. (e) Rubin, J. R.; Haromy, T. P.; Sundaralingam, M. *Acta Crystallogr.* **1991**, *C47*, 1712. (f) Waysbort, D.; Tarien, E.; Eichorn, G. L. *Inorg. Chem.* **1993**, *32*, 4774.

(3) Bear, J. L.; Gray, H. B., Jr.; Rainen, L.; Chang, I. M.; Howard, R.; Serio, S.; Kimball, A. P. *Cancer Chemother. Rep., Part 1* **1975**, *59*, 611.
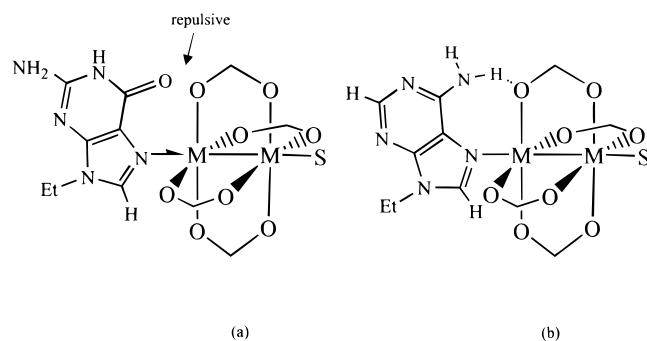
Figure 2. Interactions of DNA purines with dirhodium tetracarboxylates: (a) repulsive interactions with 9-ethylguanine, and (b) attractive interactions with 9-ethyladenine.

In recent years, additional testing has revealed that antitumor active dirhodium compounds are not limited to the tetracarboxylate species. In particular, the mixed formamidinate/carboxylate compounds such as $Rh_2(DTolF)_2(O_2CCF_3)_2(H_2O)_2$ (DTolF = N,N'-p-tolylformamidinate) (Figure 1c) are quite promising for their in vivo activity against Yoshida ascites and T8 sarcoma cells.[5] $Rh_2(DTolF)_2(O_2CCF_3)_2(H_2O)_2$ was reported to be an inhibitor of DNA synthesis and to be reactive with adenine but not guanine. In light of our recent findings in the carboxylate chemistry, we were prompted to reinvestigate the DNA nucleobase reactions of the new dirhodium formamidinate complexes. Contrary to the literature reports we have found that compounds of the type $Rh_2(form)_2(O_2CCF_3)_2$ (form = N,N'-diphenylformamidinate, N,N'-ditolylformamidinate) react with guanine as well as adenine bases via complete substitution of the trifluoroacetate ligands. Herein we report the syntheses and characterization of the products from reactions of $Rh_2(form)_2(O_2CCF_3)_2(CH_3CN)_2$ and the partially solvated compound $[Rh_2(form)_2(CH_3CN)_6][BF_4]_2$ with 9-ethyladenine (9-EtAH) and 9-ethylguanine (9-EtGH). A portion of these results has been the subject of a brief communication.[6]

Experimental Section

Starting Materials. [Rh(form)(cod)]$_2$ (cod = 1,4-cyclooctadiene) was prepared according to the literature procedure,[7a] whereas $Rh_2(form)_2(O_2CCF_3)_2(CH_3CN)_2$ and 9-EtAH were prepared by modifications of reported methods.[7b,8] 9-Ethylguanine was purchased from Sigma, and AgBF$_4$ was purchased from Aldrich; both were used without further purification. All solvents were predried over 4 Å molecular sieves with the exception of acetone and acetonitrile, which were predried over 3 Å molecular sieves. Prior to use, diethyl ether and toluene were freshly distilled from Na/K, acetone and acetonitrile were distilled over 3 Å molecular sieves, and methylene chloride was distilled from P$_2$O$_5$. Acetonitrile that was used for the electrochemical measurements was further dried by passsage through an activated alumina column under argon.

Reaction Procedures. All manipulations were performed under inert atmospheric conditions using standard Schlenk techniques unless otherwise stated.

(4) (a) Dunbar, K. R.; Matonic, J. H.; Saharan, V. P.; Crawford, C. A.; Christou, G. J. *J. Am. Chem. Soc.* **1994**, *116*, 2201. (b) Day, E. F.; Crawford, C. A.; Folting, K.; Dunbar, K. R.; Christou, G. *J. Am. Chem. Soc.* **1994**, *116*, 9339. (c) Crawford, C. A.; Day, E. F.; Saharan, V. P.; Folting, K.; Huffman, J. C.; Dunbar, K. R.; Christou, G. *Chem. Commun.* **1996**, 1113.
(5) Fimiani, V.; Ainis, T.; Cavallaro, A.; Piraino, P. *J. Chemother* **1990**, *2*, 319.
(6) Catalan, K. V.; Mindiola, D. J.; Ward, D. L.; Dunbar, K. R. *Inorg. Chem*. **1997**, *36*, 2458.
(7) (a) Piraino, P.; Tresoldi, G.; Faraone, F. *J. Organomet. Chem.* **1982**, *224*, 305. (b) Piraino, P.; Bruno, G.; Tresoldi, G.; Lo Schiavo, S.; Zanello, P. *Inorg. Chem.* **1987**, *26*, 91.
(8) Myers, T. C.; Zeleznick, L. *J. Org. Chem.* **1963**, *28*, 2087.

Rh$_2$(DTolF)$_2$(O$_2$CCF$_3$)$_2$(CH$_3$CN)$_2$ (1). A slurry of [Rh(DTolF)(cod)]$_2$ (157 mg, 0.32 mmol) in a 1:1 mixture of methanol and methylene chloride (7 mL) was treated with 3 mL of a Ag(O$_2$CCF$_3$) (281 mg, 1.3 mmol) methanol solution. The mixture was stirred for 24 h at r.t. after which time it was treated with diethyl ether to induce crystallization of the product. The red crystalline material was collected by filtration, and dried in air (204 mg, 69% yield). Purity was determined by NMR spectroscopy: ^{1}H NMR (C$_6$D$_6$) δ 1.88 (s, CH$_3$), 6.65 (d, tolyl), 6.73 (d tolyl), 7.02 (s, NCHN).

Rh$_2$(DPhF)$_2$(O$_2$CCF$_3$)$_2$(CH$_3$CN)$_2$ (2). A suspension of [Rh(DPhF)(cod)]$_2$ (350 mg, 0.8 mmol) was suspended in a 1:1 mixture of methylene chloride and methanol (14 mL) and was treated with a solution of Ag(O$_2$CCF$_3$) (751 mg, 3.4 mmol) in 7 mL methanol. The solution turned from orange to green, and after it had been stirred for 24 h at r.t. it was filtered through a Celite plug and then reduced in volume. An excess of diethyl ether was added to effect precipitation of the red product, which was collected by filtration. Purity was determined by NMR spectroscopy: ^{1}H NMR (CD$_3$CN) δ 7.05 (t, phenyl), 7.22 (s, NCHN), 7.31 (t, phenyl), 8.15 (d, phenyl).

9-Ethyladenine (9-EtAH). Adenine (828 mg, 6.13 mmol) and 2.58 g of 35% aqueous tetraethylammonium hydroxide were placed into a 50 mL round-bottomed Schlenk flask equipped with an internal condenser. The reaction mixture was stirred for 0.5 h at r.t., after which time the water was evaporated to yield an off-white residue. The residue was heated to 200 °C which resulted in the sublimation of the 9-EtAH onto the water-cooled condenser. The material was recrystallized from methylethyl ketone to yield 800 mg of purified material (80% yield). ^{1}H NMR (CD$_3$CN) δ 1.43 (t, CH$_3$), 4.17 (d, CH$_2$), 7.89 (s, H2), 8.21 (s, H8).

Rh$_2$(DTolF)$_2$(9-EtGH)$_2$(O$_2$CCF$_3$)$_2$ (3). Rh$_2$(DTolF)$_2$(O$_2$CCF$_3$)$_2$(CH$_3$CN)$_2$ (26 mg, 0.00361 mmol) was dissolved in 4 mL of CH$_3$CN, 9-EtGH (12.7 mg, 0.0071 mmol) was added to the red solution, and the mixture was refluxed for approximately 1 h. The olive-green solution was allowed to cool to room temperature, after which time it was filtered and treated with Et$_2$O to effect precipitation of the product. The green solid was washed with 20 mL of Et$_2$O and dried under reduced pressure (32 mg, 83% yield). Purity was established by NMR spectroscopy: ^{1}H NMR (CD$_3$CN) δ 1.35−1.37 (m, CH$_3$), 1.95 (s, CH$_3$CN), 2.15 (s, H$_2$O), 2.23 (s, CH$_3$), 4.05 (m, CH$_2$), 6.80 (d, tolyl), 6.89 (d, tolyl), 7.03−7.19 (m, tolyl), 7.55 (m, NCHN), 7.99 (s, H2), 8.02 (s, H8). ^{19}F NMR (both CD$_3$CN and acetone-d_6) δ −12.49 (s, O$_2$CCF$_3$) referenced to C$_6$H$_5$CF$_3$.

Rh$_2$(DPhF)$_2$(9-EtGH)$_2$(O$_2$CCF$_3$)$_2$ (4). A quantity of Rh$_2$(DPhF)$_2$(O$_2$CCF$_3$)$_2$(CH$_3$CN)$_2$ (16.8 mg, 0.00234 mmol) was dissolved in 5 mL of CH$_3$CN and 9-EtGH (9.0 mg, 0.0050 mmol) was added. The resulting red solution was refluxed for ~1 h, and the solvent was evaporated under reduced pressure to yield a dark green residue, which was recrystallized from acetone/hexanes (3 mL/5 mL) at −10 °C. The bright green solid was collected by filtration and dried in vacuo (19 mg, 79% yield). The purity was established by NMR spectroscopy: ^{1}H NMR (CD$_3$CN) δ 1.35−1.38 (m, CH$_3$), 1.95 (s, CH$_3$CN), 2.21 (s, H$_2$O), 4.04−4.07 (m, CH$_2$), 6.82 (d, phenyl), 6.89 (d, phenyl), 7.04−7.20 (m, phenyl), 7.55 (m, NCHN), 7.93 (s, H2), 8.03 (s, H8). ^{19}F NMR (CD$_3$CN and acetone-d_6) δ −12.47 (s, O$_2$CCF$_3$) referenced to C$_6$H$_5$CF$_3$. ^{103}Rh NMR (CD$_3$CN) δ 5551.98.

[Rh$_2$(DTolF)$_2$(CH$_3$CN)$_6$][BF$_4$]$_2$ (5). [Rh(cod)(DTolF)]$_2$ (97 mg, 0.15 mmol) and AgBF$_4$ (120 mg, 0.62 mmol) were dissolved in 20 mL of a 1:1 mixture of CH$_3$CN/CH$_2$Cl$_2$ in the absence of light. Within 2−3 h, the yellow-orange solution had changed to a clear, pale green color, and after 2 days visible Ag metal deposits were present. The mixture was filtered through a Celite plug, concentrated to ~5 mL under reduced pressure, treated with 3 mL of diethyl ether, and finally chilled to −10 °C. An orange-red microcrystalline solid was collected by suction filtration, washed with 3 × 5 mL portions of diethyl ether and dried in vacuo (138 mg, 93%). ^{1}H NMR (CD$_3$CN) δ 1.96 (s, ax-CH$_3$-CN), 2.27 (s, CH$_3$, tolyl), 2.49 (s, eq-CH$_3$CN), 6.99 (m, tolyl), 7.51 (t, $^3J_{Rh-H}$ = 4 Hz, NCHN). ^{103}Rh NMR (CD$_3$CN) δ 4648.

[Rh$_2$(DTolF)$_2$(9-EtAH)$_2$(CH$_3$CN)][BF$_4$]$_2$ (6). Compound **5** (60.3 mg, 0.0556 mmol) was dissolved in CH$_3$CN (2 mL) and treated with a CH$_3$CN solution (3 mL) of 9-EtAH (18.2 mg, 0.112 mmol). The mixture was stirred for ~2 days, after which time a green solid

precipitated from solution by the addition of Et_2O (5 mL); single crystals were grown from a mixture of $CH_3CN/C_6H_5CH_3$. ^1H NMR at 25 °C (CD_3CN) δ 1.25 (t, CH_3), 1.95 (s, CH_3CN), 2.25 (s, CH_3), 2.33 (s, CH_3), 3.98−4.11 (m, CH_2), 6.46 (d, tolyl), 6.76 (d, tolyl), 7.02 (d, tolyl), 7.09 (d, tolyl), 7.26 (s, NCHN), 7.68 (s, H2), 8.06 (s, H8), 8.63 (s, H6). ^1H NMR at −32 °C (CD_3CN) δ 1.28 (t, CH_3), 1.95 (s, CH_3CN), 2.13 (s, H_2O), 2.23 (s, CH_3), 4.08 (m, CH_2), 6.36 (d, tolyl), 6.46 (s, H6), 6.78 (d, tolyl), 6.96 (d, tolyl), 6.99 (d, tolyl), 7.65 (t, NCHN), 7.68 (s, H2), 8.04 (s, H8). ^1H NMR at 25 °C (acetone-d_6) δ 1.30 (t, CH_3-9-EtAH), 1.88 (s, ax-CH_3CN), 2.14 (s, H_2O), 2.24 (s, CH_3, tolyl), 4.15−4.19 (m, CH_2-9-EtAH), 6.71 (d, tolyl), 6.86 (d, tolyl), 7.06 (d, tolyl), 7.12 (d, tolyl), 7.73 (s, NCHN), 7.94 (s, H2), 8.63 (s, H8), 11.35 (s, H6). ^1H NMR at ⁻41 °C (acetone-d_6) δ 1.27 (t, CH_2-9-EtAH), 1.84 (s, ax-CH_3CN), 2.13 (s, CH_3, tolyl), 2.20 (s, CH3, tolyl), 4.17 (m, CH_2-9-EtAH), 6.76 (d, H6), 6.88 (d, tolyl), 7.03 (d, tolyl), 7.11 (d, tolyl), 7.20 (s, H1), 7.71 (s, NCHN), 7.99 (d, H2), 8.73 (s, H8), 11.57 (s, H6).

[Rh$_2$(DTolF)$_2$(9-EtGH)$_2$(CH$_3$CN)][BF$_4$]$_2$ (7). (a) A quantity of 9-ethylguanine (41.7 mg, 0.233 mmol) was added to a stirring solution of [Rh$_2$(DTolF)$_2$(CH$_3$CN)$_6$][BF$_4$]$_2$ (115.4 mg, 0.116 mmol) dissolved in 5 mL of CH_3OH and 10 mL of CH_3CN. The mixture was gently refluxed for ∼2 h, during which time the orange-red mixture with the suspended 9-ethylguanine became a clear green solution. The reaction mixture was filtered, and the filtrate was evaporated in vacuo to yield a green solid (60 mg, 47% yield).

(b) The aforementioned reaction was repeated in an acetonitrile/ acetone solvent mixture. Two equivalents of 9-EtGH (46 mg, 0.0257 mmol) were added to a solution of acetonitrile/acetone (5 mL/1 mL) of **5** (138.5 mg, 0.0129 mmol). The mixture was stirred at constant reflux for ∼3 h, filtered in air through a Celite plug, and finally reduced to dryness in vacuo (110 mg, 78% yield). ^1H NMR (CD_3OD) δ 1.36 (t, CH_3), 1.40 (t, CH_3), 1.92 (s, CH_3CN), 2.23 (s, CH_3), 3.98 (q, CH_2), 4.05 (q, CH_2), 6.80 (m, tolyl), 6.89 (m, tolyl), 7.00 (m, tolyl), 7.50 (t, NCHN), 7.55 (t, NCHN), 8.32, 8.35 (s, H8).

Physical Measurements. Infrared spectra were collected on a Nicolet 740 FT-IR spectrophotometer. All ^1H NMR spectroscopic data including the 2-dimensional experiments were collected on a either a 300 or a 500 MHz Varian spectrometer. Chemical shifts were referenced relative to the residual proton impurities of the solvents used. Electrochemical measurements were performed by using an EG&G Princeton Applied Research model 362 scanning potentiostat in conjunction with a Soltec model VP-6424S X-Y recorder. The cyclic voltammetric experiments for compound **5** were carried out r.t. in acetonitrile containing 0.1 M tetra-n-butylammonium hexafluorophosphate, TBAPF$_6$, as supporting electrolyte, while the experiments for **6** and **7** were performed with 0.1 M tetra-n-butylammonium tetrafluoroborate, TBABF$_4$, as the supporting electrolyte. $E_{1/2}$ values, determined as $(E_{p,a} + E_{p,c})/2$, were referenced to the Ag/AgCl electrode without correction for junction potentials. The Cp$_2$Fe/Cp$_2$Fe$^+$ couple occurs at $E_{1/2} = +0.46$ V, $E_{1/2} = +0.53$ V, and $E_{1/2} = +0.45$ V for the cyclic voltammograms of compounds **5**, **6**, and **7**, respectively, under the same experimental conditions in acetonitrile.

X-ray Crystallography and Structure Solution. Geometric and intensity data for compound **5** were collected on a Rigaku AFC6S diffractometer at −100 ± 1 °C. A hemisphere of crystallographic data for compound **6** was collected at −100 ± 1 °C on a Nicolet P3/V diffractometer upgraded to a Siemens P3/F with graphite-monochromated Mo Kα ($\lambda_\alpha = 0.710\ 73$ Å) radiation; the reflections were corrected for Lorentz and polarization effects. All calculations for the structure solution and the refinement of compounds **5** and **6** were performed with Silicon Graphics computers on a cluster network in the Department of Chemistry at Michigan State University using the Texsan software package of the Molecular Structure Corporation.[9] The

X-ray crystallographic data for compounds **1** and **7** were collected on a Siemens SMART diffractometer at −100 ± 1 °C with graphite monochromated Mo Kα ($\lambda_\alpha = 0.710\ 73$ Å) radiation and were corrected for Lorentz and polarization effects. Calculations were performed on a Silicon Graphics computer. The frames were integrated with the Siemens SAINT software package, and the data were corrected for absorption using the SADABS program.[10] The structures of **1** and **7** were solved by direct methods using the SHELXS program in the Bruker SHELXTL v. 5.05 software[11a] and refined by full-matrix least-squares calculations on F^2 using the SHELXL-97 program.[11b] All relevant crystallographic values and other pertinent information for compounds **1**, **5**, **6**, and **7** are listed in Tables 1−7.

Rh$_2$(DTolF)$_2$(O$_2$CCF$_3$)$_2$(CH$_3$CN)$_2$ (1). An orange-red rectangular platelet of dimensions $0.11 \times 0.31 \times 0.10$ mm was selected from a batch of crystals obtained from the evaporation of an acetonitrile solution of the compound and mounted on the tip of a glass fiber with Dow Corning grease. Indexing and refinement of 59 reflections selected from a total of 45 frames with an exposure time of 10 s/frame gave unit cell parameters for a monoclinic unit cell. A total of 1321 frames were collected with a scan width of 0.3° in ω and an exposure time of 30 s/frame. The total data collection time was 13.5 h. The integration of the frame data using a monoclinic B-centered unit cell yielded a total of 25 160 reflections in the range $h = 14 \rightarrow -14$, $k = 27 \rightarrow -28$, $l = 23 \rightarrow -15$ with a maximum 2θ angle of 56.78°. Of the 10 101 unique reflections, a total of 3761 reflections remained with $I > 2\sigma(I)$ and $R_{int} = 0.1116$ and $R_{sig} = 0.1390$ after data reduction. The positions of all of the non-hydrogen atoms were located by direct methods and refined anisotropically. Hydrogen atoms were calculated at fixed positions. Final refinement of 506 parameters and 31 restraints gave residuals of R1 = 0.0451 and wR2 = 0.0904. The goodness-of-fit was 0.717 with the maximum and minimum peak heights in the final difference Fourier map being 0.649 and −0.994 e/Å^3, respectively.

[Rh$_2$(DTolF)$_2$(CH$_3$CN)$_6$][BF$_4$]$_2$ (5). Large single crystals were obtained from the slow diffusion of a concentrated acetonitrile solution of the compound into toluene. The crystals grew as long orange-red rectangles at the interface of the two solvents after 12 days. A suitable single crystal, with the approximate dimensions $0.78 \times 0.26 \times 0.21$ mm, was mounted on the tip of a glass fiber with Dow Corning grease and cooled in a liquid nitrogen stream. Cell constants for an orthorhombic unit cell were obtained from a least squares refinement using 24 carefully centered reflections in the range $29 < 2\theta < 37°$. The reflection data were collected in the range $4 \le 2\theta \le 47°$, by using the ω scan method. Weak reflections (those with $F < 10\sigma(F)$) were rescanned a maximum of 3 times, and the counts were accumulated to ensure good counting statistics. Of the 8005 reflections which were collected, 3865 reflections with $F_o^2 > 3\sigma(F_o)^2$ were used in the measurement. Periodic measurement of three representative reflections at regular intervals revealed that no loss of diffraction intensity had occurred during data collection. An empirical absorption correction was applied on the basis of azimuthal scans of 3 reflections with χ near 90°. The space group was determined to be *Pbca* on the basis of the observed systematic absences. The positions of all non-hydrogen atoms were obtained by the application of the direct methods programs MITHRIL and DIRDIF followed by successive full-matrix least-squares cycles[9] and refined with anisotropic thermal parameters. Hydrogen atoms were treated as fixed contributors at idealized positions and were not refined. Final least-squares refinement of 567 parameters resulted in residuals of $R = 0.046$ and $R_w = 0.063$ and a goodness-of-fit = 2.01. A final difference Fourier map revealed the highest peak to be 0.87 e$^-$/Å^3.

[Rh$_2$(DTolF)$_2$(9-EtAH)$_2$(CH$_3$CN)][BF$_4$]$_2$ (6). Single X-ray quality crystals of **6** were grown from the slow diffusion of an acetonitrile solution of **6** into toluene. A green rectangular crystal of approximate dimensions of $0.31 \times 0.23 \times 0.18$ mm was mounted on the tip of a glass fiber with Dow Corning grease. Cell constants for the monoclinic space group $P2_1/c$ were obtained from a least-squares refinement of

(9) (a) *TEXSAN−TEXRAY Structure Analysis Package*; Molecular Structure Corporation: The Woodlands, TX, 1985. (b) MITHRIL: Integrated Direct Methods Computer Program, Gilmore, C. J. *J. Appl. Crystallogr.* **1984**, *17*, 42. (c) P. T. DIRDIF: Direct Methods for Difference Structures, An Automatic Procedure for Phase Extension; Refinement of Difference Structure Factors; Beurskens, Technical Report, 1984.

(10) SAINT & SADABS programs in the SHELXTL software, Bruker AXS, Inc., Analytical X-ray Systems.
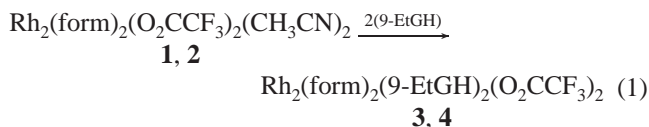
(11) (a) Sheldrick, G. *SHELXS-97*; University of Göttingen: Göttingen, 1990. (b) Sheldrick, G. *SHELXL-97*; 1997.

25 carefully centered reflections in the range $15 < 2\theta < 21°$. The data were collected using the $\omega-2\theta$ scan technique to a maximum 2θ value of 45° in the range $4 < 2\theta < 45°$. Of the 7151 reflections that were collected, 6841 were unique with $R_{int} = 0.119$. Standards collected every 150 reflections during the data collection revealed no significant decrease in diffraction intensity. An empirical absorption correction was applied on the basis of azimuthal scans of 3 reflections with χ near 90°. The structure was solved by direct methods using the MITHRIL program and expanded using Fourier techniques. The ethyl carbon atoms of the 9-EtAH molecules and the aromatic carbon atoms of the DTolF groups were refined isotropically while the remaining non-hydrogen atoms were refined anisotropically. All hydrogen atoms were calculated at fixed positions. The final least-squares refinement of 503 parameters based on 2240 observed reflections ($I > 3.00\sigma(I)$) resulted in residuals of $R = 0.063$ and $R_w = 0.073$ and a goodness-of-fit = 1.30. A final difference Fourier map revealed the highest peak to be 0.75 e$^-$/Å^3 and the minimum peak height to be -0.65 e$^-$/Å^3.

[Rh$_2$(DTolF)$_2$(9-EtAH)$_2$(CH$_3$CN)](BF$_4$)$_2$ (7). A green prismatic platelet having dimensions $0.10 \times 0.065 \times 0.078$ mm was obtained from the evaporation of a methylene chloride solution. The selected crystal, which was quite small and soft, was mounted on the tip of a glass fiber with Dow Corning grease. A total of 1321 reflections were collected with a scan width of 0.3° in ω and an exposure time of 44 s/frame from which 107 reflections were used for indexing a triclinic cell. The data were integrated to yield a total of 31 002 reflections in the range $h = 13 \rightarrow -14$, $k = 24 \rightarrow -27$, $l = 19 \rightarrow -29$ with a maximum 2θ angle of 56.68°. After data reduction of the 12 287 unique reflections, 4,834 reflections remained with $I > 2\sigma(I)$. The R_{int} and R_{sig} values were 0.1480 and 0.2539, respectively. These fairly high residuals are indicative of the poor quality of the crystal. The positions of the Rh atoms were located by direct methods and the remaining non-hydrogen atoms were located through successive cycles of least-squares refinements and difference Fourier maps. A disordered [BF$_4$]$^-$ anion was located and modeled with partial occupancy distributed over two positions. All of the nonhydrogen atoms of the cationic complex and one of the [BF$_4$]$^-$ anions were refined anisotropically. The F atoms of the disordered [BF$_4$]$^-$ anion were refined anisotropically while the B atom was refined isotropically with a constraint on the temperature factor. The hydrogen atoms were refined at fixed positions. The final full-matrix least-squares on F^2 revealed maximum and minimum peak heights of 1.43 and -0.732 e$^-$/Å^3 with final residuals of R1 = 0.0898 and wR2 = 0.1484 for 694 parameters and 95 restraints. The final goodness-of-fit was 0.974.
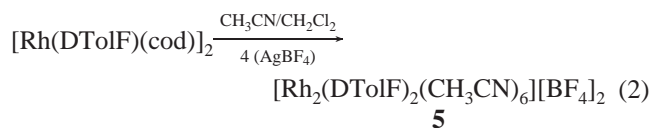
Results and Discussion.

Syntheses. Our modified syntheses of the antitumor active compound Rh$_2$(DTolF)$_2$(O$_2$CCF$_3$)$_2$(H$_2$O)$_2$ in acetonitrile or methanol rather than water led to the isolation of the new axial adducts Rh$_2$(form)(O$_2$CCF$_3$)$_2$L$_2$ (**1** and **2**, L = CH$_3$CN or CH$_3$-OH) in greater yields and a higher purity.[7b] Both **1** and **2** react with 2 equiv of 9-EtGH to yield Rh$_2$(DTolF)$_2$(9-EtGH)$_2$(O$_2$-CCF$_3$)$_2$ (**3**) and Rh$_2$(DPhF)$_2$(9-EtGH)$_2$(O$_2$CCF$_3$)$_2$ (**4**) (eq 1). The use of refluxing conditions serves to increase the solubility of the 9-EtGH which enhances the rate of the reaction.
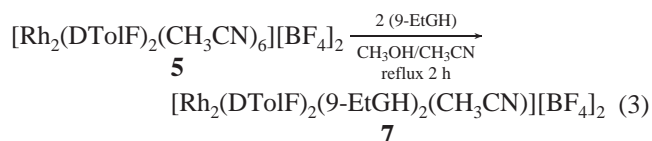
$$\text{Rh}_2(\text{form})_2(\text{O}_2\text{CCF}_3)_2(\text{CH}_3\text{CN})_2 \xrightarrow{2(9\text{-EtGH})}$$
$$\textbf{1, 2}$$
$$\text{Rh}_2(\text{form})_2(9\text{-EtGH})_2(\text{O}_2\text{CCF}_3)_2 \quad (1)$$
$$\textbf{3, 4}$$

Reports that the bridging trifluoroacetate groups of Rh$_2$-(DTolF)$_2$(O$_2$CCF$_3$)$_2$(H$_2$O)$_2$ exhibit increased lability due to the strong trans influence of the [DTolF]$^-$ ligands prompted us to investigate the preparation of the partially solvated dication [Rh$_2$(DTolF)$_2$(CH$_3$CN)$_6$]$^{2+}$ (**5**) to complement our studies involving **1** and **2**.[12] The ^{19}F NMR spectra (Table 9) for **1** and **2** in donating solvents such as acetonitrile revealed that the trifluoroacetate anions were uncoordinated, thus it seemed

highly likely that this compound would be accessible. In addition, our earlier preparation of the analogous diiridium complex [Ir$_2$(DTolF)$_2$(CH$_3$CN)$_6$][BF$_4$]$_2$ lent further credence to the idea.[13] The reaction of [Rh(cod)(DTolF)]$_2$ with 4 equiv of AgBF$_4$ in CH$_3$CN affords [Rh$_2$(DTolF)$_2$(CH$_3$CN)$_6$]$^{2+}$ (**5**) in high yields (eq 2).

$$[\text{Rh}(\text{DTolF})(\text{cod})]_2 \xrightarrow[4 (\text{AgBF}_4)]{\text{CH}_3\text{CN/CH}_2\text{Cl}_2}$$
$$[\text{Rh}_2(\text{DTolF})_2(\text{CH}_3\text{CN})_6][\text{BF}_4]_2 \quad (2)$$
$$\textbf{5}$$

[Rh$_2$(DTolF)$_2$(CH$_3$CN)$_6$][BF$_4$]$_2$ reacts with 2 equiv of 9-EtGH in refluxing methanol/acetonitrile to yield two isomers of [Rh$_2$-(DTolF)$_2$(9-EtGH)$_2$(CH$_3$CN)][BF$_4$]$_2$ (eq 3) as judged by the ^{1}H NMR spectrum (*vide infra*).

$$[\text{Rh}_2(\text{DTolF})_2(\text{CH}_3\text{CN})_6][\text{BF}_4]_2 \xrightarrow[\substack{\text{CH}_3\text{OH/CH}_3\text{CN} \\ \text{reflux 2 h}}]{2 (9\text{-EtGH})}$$
$$\textbf{5}$$
$$[\text{Rh}_2(\text{DTolF})_2(9\text{-EtGH})_2(\text{CH}_3\text{CN})][\text{BF}_4]_2 \quad (3)$$
$$\textbf{7}$$

The formation of two compounds with the same composition but with different arrangements of the purines had been previously observed in the chemistry of Rh$_2$(O$_2$CCH$_3$)$_4$ and [Rh$_2$(O$_2$CCH$_3$)$_2$(CH$_3$CN)$_6$][BF$_4$]$_2$ with 9-ethylguanine. [Rh$_2$-(DTolF)$_2$(CH$_3$CN)$_6$][BF$_4$]$_2$ reacts with two equivalents of 9-EtAH in acetonitrile at r.t. (eq 4), but in this case only one isomer is formed, namely [Rh$_2$(DTolF)$_2$(9-EtAH)$_2$(CH$_3$CN)]-[BF$_4$]$_2$ as Et-judged by ^{1}H NMR spectroscopy.

$$[\text{Rh}_2(\text{DTolF})_2(\text{CH}_3\text{CN})_6][\text{BF}_4]_2 \xrightarrow{2 (9\text{-EtAH})}$$
$$\textbf{5}$$
$$[\text{Rh}_2(\text{DTolF})_2(9\text{-EtAH})_2(\text{CH}_3\text{CN})][\text{BF}_4]_2 \quad (4)$$
$$\textbf{6}$$
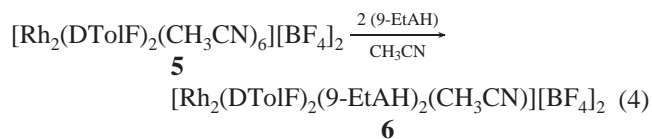
Description of Structures. ORTEP representations of the cations in compounds **1**, **5**, **6**, and a PLUTO of **7** are depicted in Figures 3, 4, 5, and 6, respectively; fractional coordinates and selected metrical parameters are listed in Tables 1−7.

Rh$_2$(DTolF)$_2$(O$_2$CCF$_3$)$_2$(CH$_3$CN)$_2$ (1). Substitution of the water molecules in the axial positions of Rh$_2$(DTolF)$_2$(O$_2$CCF$_3$)$_2$ with CH$_3$CN results in subtle changes in the lantern structure of the mixed-ligand complex. An ORTEP representation of **1** which crystallizes in the monoclinic space group $P2_1/n$ is presented in Figure 3. The dirhodium core consists of two cis [DTolF]$^-$ ligands and two [O$_2$CCF$_3$]$^-$ ligands. The geometry around the Rh atoms is essentially octahedral with a Rh−Rh bond length of 2.4743(5) Å. This distance is longer than the corresponding value observed for the bis-water adduct (Rh−Rh = 2.425(1) Å).[7b] The lengthening of the metal−metal bond is attributed to the stronger interactions of the axial acetonitrile molecules (Rh(1)−N(3) = 2.267(5) Å and Rh(2)−N(4) = 2.265(5) Å). Interestingly, both axial acetonitriles are coordinated at angles significantly less than 180°, with Rh(1)−Rh(2)−N(4) and Rh(2)−Rh(1)−N(3) angles of 172.37(11)° and 168.88(11)°. The bis-water adduct exhibits similar bends for the axial water molecules (∠Rh−Rh−O$_{av}$ =168.6(1)°), and the compound [Rh$_2$(DTolF)$_2$(bpy)(CH$_3$CN)$_4$][BF$_4$]$_2$ exhibits an axial acetonitrile ligand coordinated at an even more acute angle of

(12) (a) Piraino, P.; Tresoldi, G.; Schiavo, S. L. *Inorg. Chim. Acta* **1993**, *203*, 101. (b) Schiavo, S. L.; Sinicropi, M. S.; Tresoldi, G.; Arena, C. G.; Piraino, P. *J. Chem. Soc., Dalton Trans.* **1994**, 1517 and references therein.

(13) Dunbar, K. R.; Majors, S. O.; Sun, J.-S. *Inorg. Chim. Acta* **1995**, *229*, 373.

Table 1. Crystallographic Data for
Rh$_2$(DTolF)$_2$(O$_2$CCF$_3$)$_2$(CH$_3$CN)$_2$ (**1**), [Rh$_2$(DTolF)$_2$(CH$_3$CN)$_6$][BF$_4$]$_2$
(**5**), and [Rh$_2$(DTolF)$_2$(9-EtAH)$_2$(CH$_3$CN)][BF$_4$]$_2$ (**6**)

	1	5	6
formula^a	C$_{38}$H$_{36}$F$_6$N$_6$O$_4$Rh$_2$	C$_{42}$H$_{60}$B$_2$F$_8$N$_{10}$Rh$_2$	C$_{46}$H$_{48}$B$_2$F$_8$N$_{15}$Rh$_2$
fw, g/mol	960.55	1084.42	1190.40
cryst syst	monoclinic	orthorhombic	monoclinic
space group	$P2_1/n$	$Pcba$	$P2_1/c$
a/Å	10.8495(3)	21.646(3)	15.648(8)
b/Å	21.4349(6)	31.272(3)	16.515(5)
c/Å	18.6766(3)	14.561(4)	20.026(8)
α/deg	90	90	90
β/deg	90.059(1)	90	105.17(4)
γ/deg	90	90	90
V/Å^3	4340.6(2)	9857(3)	4994(6)
Z	4	8	4
T/°C	−100	−100	−100
D$_c$, g/cm^{-3}	1.470	1.461	1.583
μ_{Mo}/cm^{-1}	8.29	7.39	7.40
N	10101	8005	6841
N_o ^{b}	3761	3862^g	2240^g
R^c (R_{sig})	0.118 (0.191)		0.119
R_w ^{d}	0.045 (0.090)	0.042^h (0.045)^i	0.063^h (0.073)^i

^{a} Including solvent molecules. ^{b} $I > 2\sigma(I)$. ^{c} $R = \sum|F_o{}^2 - F_o{}^2(\text{mean})|/\sum[F_o{}^2]$; $R_{sig} = \sum[\sigma(F_o{}^2)]/[F_o{}^2]$. ^{d} $R_w = \sum||F_o| - |F_c||/\sum|F_o|$; wR2 $= [\sum[w(F_o{}^2 - F_c{}^2)^2]/\sum[w(F_o{}^2)^2]]^{1/2}$. ^{g} $F_o{}^2 > 3\sigma(F_o)^2$. ^{h} $R = \sum||F_o| - |F_c||/\sum|F_o|$. ^{i} $R_w = [\sum w(|F_o| - |F_c|^2/\sum w|F_o|^2]^{1/2}$; $w = 1/\sigma^2(|F_o|)$.

161.9(26)°.[14] The average Rh−O bond distance (2.098(3) Å) of the coordinated trifluoroacetate groups in **1** is slightly longer than the average Rh−O distance reported for the bis-water adduct (2.083(3) Å). The O−C−O angles of the trifluoroacetate groups are 129.7(5)° and 131.4(5)° for O(1)−C(28)−O(3) and O(2)−C(31)−O(4), respectively. The [O$_2$CCF$_3$]$^-$ groups are twisted by 5.32(13)° and 6.03(14)° from the eclipsed orientation in comparison to 8.0(1)° and 8.3(1)° twists of the [O$_2$CCF$_3$]$^-$ bridges in the bis-water adduct. Distances involving the [DTolF]$^-$ groups (e.g. the average Rh−N distance of 2.011(4) Å) are within normal ranges. Likewise, the N−C−N angles of the bridgehead C atoms of 124.4(5)° and 125.8(5)° are in expected ranges. The [DTolF]$^-$ groups are slightly twisted from the eclipsed orientation by 5.4(2)° and 5.6(2)° in comparison to the greater twists reported for the bis-water adduct of 9.4-(2)° and 9.5(2)°.

[Rh$_2$(DTolF)$_2$(CH$_3$CN)$_6$][BF$_4$]$_2$ (5). The partially solvated complex, [Rh$_2$(DTolF)$_2$(CH$_3$CN)$_6$][BF$_4$]$_2$ is isomorphic to the related compound [Ir$_2$(DTolF)$_2$(CH$_3$CN)$_6$][BF$_4$]$_2$ prepared in our laboratories several years ago.[13] An ORTEP representation of the dirhodium cation is depicted in Figure 4. Both compounds exhibit a C_{2v} symmetry and crystallize in the orthorhombic space group *Pbca* with cis, bridging [DTolF]$^-$ groups and CH$_3$CN in the remaining six metal coordination sites. The average Rh−N is 2.042(7) Å is not statistically different than the corresponding distance in the Ir analogue of 2.05(1) Å. These values are longer than the corresponding distances in the bis-trifluoroacetate derivatives, however, and the [DTolF]$^-$ ligands are twisted by ∼19° from the eclipsed orientation (compared to a 20° twist in [Ir$_2$(DTolF)$_2$(CH$_3$CN)$_6$]$^{2+}$). These are significantly greater distortions than what was observed for the bis-trifluoroacetate derivatives, but it is not particularly unusual for compounds of this structural type.[15] The angles subtended by the N−C−N bridgehead in the five-membered rings are within normal ranges (1235.2(6)° and 123.4(7)°). The remaining equatorial positions

(14) Catalan, K. V.; Dunbar, K. R.; Maloney, M. M. Manuscript in preparation.

(15) Cotton, F. A.; Walton, R. A. *Multiple Bonds between Metal Atoms*, 2nd ed.; Oxford University Press: Oxford, 1993, and references therein.

Table 2. Positional Parameters and Equivalent Isotropic Thermal Parameters for Rh$_2$(DTolF)$_2$(O$_2$CCF$_3$)$_2$(CH$_3$CN)$_2$ (**1**)

atom	x	y	z	U_{eq}
Rh1	0.0265(1)	0.1968(1)	0.316212)	0.047(1)
Rh2	0.056214)	0.1972(1)	0.4482(1)	0.046(1)
O1	−0.0201(3)	0.2871(2)	0.4465(2)	0.057(1)
O2	0.1986(3)	0.2412(2)	0.3115(2)	0.057(1)
O3	−0.0649(3)	0.2821(1)	0.3278(2)	0.056(1)
O4	0.2330(3)	0.2332(2)	0.4321(2)	0.058(1)
N1	−0.1359(4)	0.1542(2)	0.3295(2)	0.049(1)
N2	−0.1155(4)	0.1628(2)	0.4544(2)	0.050(1)
N3	−0.0008(5)	0.2169(2)	0.1976(3)	0.064(1)
N4	0.1059(4)	0.2055(2)	0.5667(2)	0.058(1)
N5	0.1157(4)	0.1144(2)	0.3142(2)	0.052(1)
N6	0.1280(4)	0.1111(2)	0.4400(2)	0.054(1)
C1	−0.4612(7)	0.1016(4)	0.0867(4)	0.122(3)
C2	0.1900(9)	−0.0165(4)	0.0482(4)	0.164(4)
C4	0.3873(6)	−0.0017(3)	0.6800(3)	0.109(3)
C5	−0.2581(7)	0.0933(3)	0.1543(3)	0.082(2)
C6	−0.4127(6)	0.1505(3)	0.2076(4)	0.082(2)
C7	−0.3750(7)	0.1154(3)	0.1509(4)	0.078(2)
C8	−0.1795(6)	0.1055(3)	0.2132(3)	0.072(2)
C9	0.1440(6)	0.1976(3)	0.6235(3)	0.066(2)
C10	0.1924(7)	0.0282(3)	0.6129(3)	0.067(2)
C11	0.1704(7)	0.0176(4)	0.1196(3)	0.097(2)
C12	0.1934(7)	0.1853(3)	0.6954(3)	0.104(3)
C13	0.1226(6)	−0.0116(3)	0.1784(4)	0.088(2)
C15	0.2040(6)	0.0792(3)	0.1282(3)	0.094(2)
C16	−0.0155(6)	0.2323(3)	0.1405(4)	0.087(2)
C17	0.1891(5)	0.1100(3)	0.1917(3)	0.070(2)
C18	−0.0373(8)	0.2517(5)	0.0645(4)	0.177(4)
C19	−0.2805(5)	0.0850(2)	0.6024(3)	0.057(1)
C20	0.3175(6)	0.0802(2)	0.5031(3)	0.067(2)
C21	−0.2866(5)	0.1318(2)	0.6540(3)	0.053(1)
C22	0.3796(6)	0.0524(3)	0.5603(4)	0.081(2)
C23	0.1049(6)	0.0188(3)	0.2433(3)	0.072(2)
C24	0.1293(5)	0.0553(3)	0.5559(3)	0.061(2)
C25	−0.3516(6)	0.1209(2)	0.7230(3)	0.076(2)
C27	−0.3374(6)	0.1638(2)	0.2665(3)	0.064(2)
C28	−0.0663(5)	0.3061(2)	0.3884(3)	0.057(1)
C29	0.3183(7)	0.0274(3)	0.6166(3)	0.068(2)
C30	−0.1798(5)	0.1990(2)	0.5724(3)	0.053(1)
C31	0.2589(5)	0.2466(2)	0.3686(3)	0.056(2)
C32	0.1376(5)	0.0802(3)	0.2499(3)	0.056(2)
C33	−0.2184(6)	0.1414(2)	0.2699(3)	0.054(1)
C34	0.1928(6)	0.0820(3)	0.4992(3)	0.052(1)
C35	−0.2239(5)	0.0942(2)	0.5372(3)	0.050(1)
C36	−0.2350(5)	0.1887(2)	0.6368(3)	0.057(2)
C37	−0.1738(5)	0.1516(2)	0.5211(3)	0.047(1)
C39	0.1492(5)	0.0884(2)	0.3756(3)	0.056(2)
C40	−0.1773(5)	0.1469(2)	0.3954(3)	0.054(1)
F4	−0.0596(9)	0.4117(3)	0.4028(6)	0.289(6)
F1	0.4726(4)	0.2370(2)	0.3926(2)	0.126(2)
F2	0.4232(4)	0.2828(2)	0.2978(2)	0.137(2)
F3	0.4026(4)	0.3259(2)	0.3976(3)	0.149(2)
C41	0.3894(7)	0.2729(4)	0.3626(4)	0.081(2)
C3	−0.1393(13)	0.3650(4)	0.3900(5)	0.148(5)
F5	−0.1890(9)	0.3758(4)	0.4468(4)	0.254(5)
F6	−0.1891(7)	0.3843(3)	0.3389(3)	0.240(4)

are coordinated by acetonitrile molecules with average Rh−N bond distances of 2.029(7) Å which is approximately 0.02 Å shorter than the metal-formamidinate distances. The axial Rh−NCCH$_3$ interactions of 2.235(7) and 2.208(7) Å are comparable to the distance of 2.232(4) Å reported for the related compound [Rh$_2$(O$_2$CCH$_3$)$_2$(CH$_3$CN)$_6$][BF$_4$]$_2$.[16] By comparison, [Ir$_2$(DTolF)$_2$(CH$_3$CN)$_6$][BF$_4$]$_2$ exhibits axial and equatorial Ir−NCCH$_3$ distances of 2.17(1) and 2.00(1) Å, respectively. The Rh−Rh bond distance is 2.5594(8) Å which is 0.1 Å longer than the corresponding metal−metal bond distances in related

(16) Pimblett, G.; Garner, C. D.; Clegg, W. *J. Chem. Soc., Dalton Trans.* **1986**, 1257.

Table 3. Positional Parameters and Equivalent Isotropic Thermal Parameters for [Rh$_2$(DTolF)$_2$(CH$_3$CN)$_6$][BF$_4$]$_2$ (**5**)

atom	x	y	z	B_{eq}[a]
Rh(1)	0.56796(3)	0.14524(2)	−0.03818(2)	1.82(1)
Rh(2)	0.63806(3)	0.14887(2)	0.10314(4)	1.82(1)
N(1)	0.6157(3)	0.0906(2)	−0.0677(4)	2.1(2)
N(2)	0.6942(3)	0.1081(2)	0.0345(4)	2.0(1)
N(3)	0.5080(3)	0.1112(2)	0.0410(4)	1.9(1)
N(4)	0.5867(3)	0.0991(2)	0.1470(4)	1.9(2)
N(5)	0.5238(3)	0.2007(2)	−0.0081(4)	2.2(2)
N(6)	0.5823(3)	0.1883(2)	0.1752(4)	2.4(2)
N(7)	0.6280(3)	0.1768(2)	−0.1199(5)	3.0(2)
N(8)	0.6865(3)	0.1999(2)	0.0574(4)	2.4(2)
N(9)	0.5120(3)	0.1410(2)	−0.1668(4)	2.4(2)
N(10)	0.7011(3)	0.1503(2)	0.2223(4)	2.4(2)
C(1)	0.6725(4)	0.0861(3)	−0.0355(5)	2.2(2)
C(2)	0.5314(4)	0.0909(3)	0.1133(5)	2.1(2)
C(3)	0.7170(4)	0.2279(3)	0.0359(6)	2.9(2)
C(4)	0.5577(5)	0.2106(3)	0.2216(6)	3.8(3)
C(5)	0.6566(5)	0.1926(4)	−0.1762(7)	5.2(3)
C(6)	0.4953(4)	0.2302(3)	0.0018(6)	2.8(2)
C(7)	0.7561(5)	0.2636(3)	0.0076(7)	5.3(3)
C(8)	0.6912(6)	0.2128(6)	−0.2494(8)	12.7(5)
C(9)	0.7831(4)	0.1485(3)	0.2763(5)	2.9(2)
C(10)	0.7854(5)	0.1447(4)	0.3471(7)	5.5(3)
C(11)	0.4100(4)	0.1299(3)	−0.0296(6)	2.6(2)
C(12)	0.3511(4)	0.1197(3)	−0.0601(5)	2.9(2)
C(13)	0.6090(4)	0.0696(3)	0.2156(5)	2.0(2)
C(14)	0.6232(4)	0.0278(3)	0.1919(6)	2.7(2)
C(15)	0.6448(4)	−0.0002(3)	0.2578(7)	3.4(2)
C(16)	0.6494(4)	0.0108(3)	0.3486(7)	3.8(2)
C(17)	0.6343(4)	0.0531(3)	0.3718(6)	3.6(2)
C(18)	0.6141(5)	0.0821(3)	0.3072(5)	2.2(2)
C(19)	0.6712(6)	−0.0205(4)	0.4188(8)	6.5(3)
C(20)	0.7584(4)	0.1028(3)	0.0608(5)	2.0(2)
C(21)	0.8019(4)	0.1292(3)	0.0234(6)	3.0(2)
C(22)	0.8628(4)	0.1269(3)	0.0555(7)	3.9(2)
C(23)	0.8798(4)	0.0989(3)	0.1244(7)	3.6(3)
C(24)	0.8353(4)	0.0714(3)	0.1571(6)	3.6(2)
C(25)	0.7744(4)	0.0734(3)	0.1274(6)	2.6(2)
C(26)	0.9445(5)	0.0990(4)	0.1625(8)	6.7(4)
C(27)	0.4465(4)	0.1002(3)	0.0142(5)	2.2(2)
C(28)	0.4214(5)	0.0593(3)	0.0284(6)	2.8(2)
C(29)	0.3617(4)	0.0499(3)	−0.0008(6)	3.0(2)
C(30)	0.3257(4)	0.0794(3)	−0.0460(6)	3.1(2)
C(31)	0.2613(4)	0.0683(4)	−0.0786(7)	4.7(3)
C(32)	0.4870(4)	0.1359(3)	−0.2345(6)	2.7(2)
C(33)	0.4529(5)	0.1283(5)	−0.3205(6)	4.9(3)
C(34)	0.5993(4)	0.0685(3)	−0.1501(5)	1.9(2)
C(35)	0.5464(4)	0.0436(2)	−0.1518(5)	2.2(2)
C(36)	0.5265(4)	0.0261(3)	−0.2337(6)	2.7(2)
C(37)	0.5569(4)	0.0320(3)	−0.3141(6)	3.2(2)
C(38)	0.6106(4)	0.0558(4)	−0.3118(6)	4.5(3)
C(39)	0.6325(4)	0.0737(3)	−0.2302(6)	4.0(3)
C(40)	0.5276(5)	0.2414(4)	0.2821(8)	8.2(4)
C(41)	0.4575(5)	0.2684(5)	0.0146(8)	5.4(3)
C(42)	0.5332(5)	0.0153(3)	−0.4046(7)	4.8(3)

[a] $B_{eq} = (8/3)\pi^2(U_{11}(aa^*)^2 + U_{22}(bb^*)^2 + U_{33}(cc^*)^2 + 2U_{12}aa^*bb^* \cos \gamma) + 2U_{13}aa^*cc^* \cos \beta) + 2U_{23}bb^*cc^* \cos \alpha)$.

bis-trifluoroacetate compounds, but is quite similar to the Rh−Rh distance of 2.534(1) Å in [Rh$_2$(O$_2$CCH$_3$)$_2$(CH$_3$CN)$_6$]$^{2+}$.[16] Likewise the Ir−Ir distance in [Ir$_2$(DTolF)$_2$(CH$_3$CN)$_6$]$^{2+}$ of 2.601(1) Å is longer than what is observed for Ir$_2$(DTolF)$_4$ (Ir−Ir = 2.524(3) Å). Several factors are expected to contribute to a lengthening of the M−M bond in the nitrile compounds as compared to the carboxylate derivatives, including the presence of only two bridging ligands versus four as well as the cationic charge on the compounds.

[Rh$_2$(DTolF)$_2$(9-EtAH)$_2$(CH$_3$CN)][BF$_4$]$_2$ (6). This compound crystallizes in the monoclinic space group $P2_1/c$ with the asymmetric unit consisting of the entire cation and two [BF$_4$]$^−$ anions (Figure 5). The dinuclear cation contains two

Table 4. Positional Parameters and Equivalent Isotropic Thermal Parameters for [Rh$_2$(DTolF)$_2$(9-EtAH)$_2$(CH$_3$CN)][BF$_4$]$_2$ (**6**)

atom	x	y	z	B_{eq}[a]
Rh(1)	0.7682(1)	0.1470(1)	0.1467(1)	2.52(5)
Rh(2)	0.7122(1)	0.2177(1)	0.2378(1)	2.60(5)
N(1)	0.872(1)	0.122(1)	0.230(1)	3.2(6)
N(2)	0.662(1)	0.173(1)	0.0662(10)	3.2(6)
N(3)	0.696(1)	0.050(1)	0.1685(8)	2.1(5)
N(4)	0.833(1)	0.245(1)	0.128(1)	3.1(6)
N(5)	0.806(1)	0.078(1)	0.074(1)	2.9(6)
N(6)	0.641(1)	0.302(1)	0.173(1)	3.2(6)
N(7)	0.609(1)	0.142(1)	0.2107(9)	3.0(5)
N(8)	0.815(1)	0.296(1)	0.2712(10)	3.1(5)
N(9)	0.781(1)	0.132(1)	0.303(1)	3.2(5)
N(10)	0.930(2)	0.388(1)	0.267(1)	6.2(8)
N(11)	0.991(2)	0.412(2)	0.174(2)	8(1)
N(12)	0.928(2)	0.320(1)	0.081(1)	5.6(8)
N(13)	0.542(1)	0.242(1)	−0.009(1)	4.3(7)
N(14)	0.475(2)	0.361(2)	0.023(2)	6.5(9)
N(15)	0.543(2)	0.400(2)	0.139(2)	6.0(8)
C(1)	0.856(2)	0.104(1)	0.291(1)	3.3(7)
C(2)	0.617(2)	0.069(1)	0.183(1)	3.7(8)
C(3)	0.965(2)	0.123(1)	0.233(1)	2.5(6)
C(4)	1.028(2)	0.142(2)	0.296(1)	4.4(6)
C(5)	1.117(2)	0.125(2)	0.300(1)	4.5(6)
C(6)	1.147(2)	0.099(2)	0.245(1)	4.3(6)
C(7)	1.089(2)	0.091(1)	0.183(1)	3.3(5)
C(8)	0.998(2)	0.102(1)	0.176(1)	3.4(5)
C(9)	1.244(2)	0.076(2)	0.257(2)	6.8(8)
C(10)	0.761(1)	0.100(1)	0.362(1)	3.1(7)
C(11)	0.728(1)	0.155(2)	0.405(1)	3.3(5)
C(12)	0.711(2)	0.125(1)	0.463(1)	3.7(6)
C(13)	0.728(2)	0.043(2)	0.487(1)	3.6(6)
C(14)	0.762(2)	−0.010(2)	0.444(1)	5.0(7)
C(15)	0.776(2)	0.022(2)	0.381(1)	3.8(6)
C(16)	0.714(2)	0.016(2)	0.555(1)	6.0(7)
C(17)	0.521(1)	0.166(1)	0.205(1)	2.8(5)
C(18)	0.449(1)	0.146(1)	0.150(1)	3.0(5)
C(19)	0.352(2)	0.237(2)	0.192(1)	4.6(6)
C(20)	0.424(2)	0.258(1)	0.246(1)	3.5(5)
C(21)	0.507(2)	0.223(2)	0.253(1)	3.7(5)
C(22)	0.260(2)	0.280(2)	0.180(1)	6.4(7)
C(23)	0.703(1)	−0.029(1)	0.139(1)	2.3(5)
C(24)	0.778(2)	−0.073(1)	0.169(1)	3.4(5)
C(25)	0.793(2)	−0.146(2)	0.140(1)	4.3(6)
C(26)	0.736(2)	−0.175(1)	0.083(1)	3.6(S)
C(27)	0.660(2)	−0.130(2)	0.054(1)	4.8(6)
C(28)	0.645(2)	−0.056(1)	0.083(1)	3.2(5)
C(29)	0.754(2)	−0.253(2)	0.047(1)	6.1(7)
C(30)	0.814(2)	0.037(2)	0.030(2)	3.8(8)
C(31)	0.828(2)	−0.020(2)	−0.028(2)	6.4(7)
C(32)	0.872(2)	0.329(2)	0.240(1)	4.0(9)
C(33)	0.985(2)	0.425(2)	0.232(3)	9(1)
C(34)	0.935(2)	0.353(2)	0.147(2)	5.6(9)
C(35)	0.876(2)	0.306(2)	0.172(2)	3.4(7)
C(36)	0.867(2)	0.255(1)	0.075(1)	3.6(7)
C(37)	0.969(3)	0.363(3)	0.021(2)	10(1)
C(38)	1.049(3)	0.340(2)	0.045(2)	9.6(9)
C(39)	0.607(2)	0.231(2)	0.058(2)	3.5(8)
C(40)	0.485(2)	0.306(2)	−0.021(2)	6(1)
C(41)	0.536(2)	0.352(2)	0.084(2)	5.2(9)
C(42)	0.599(2)	0.293(2)	0.105(2)	2.9(7)
C(43)	0.607(2)	0.370(2)	0.192(1)	3.9(8)
C(44)	0.472(3)	0.466(3)	0.151(2)	11(1)
C(45)	0.509(3)	0.530(3)	0.143(2)	13(1)
C(46)	0.365(2)	0.184(1)	0.146(1)	4.1(6)
B(1)	0.975(2)	0.148(3)	−0.055(2)	5(1)
B(2*)	0.615(5)	0.410(2)	0.384(3)	10(2)
F(1)	0.979(1)	0.079(1)	−0.0904(9)	8.0(6)
F(2)	1.004(1)	0.141(1)	0.0129(8)	7.8(6)
F(3)	1.018(1)	0.210(1)	−0.0819(10)	8.2(6)
F(4)	0.885(1)	0.172(1)	−0.0722(8)	7.5(6)
F(5*)	0.676(2)	0.376(2)	0.366(1)	17(1)
F(6*)	0.569(2)	0.339(2)	0.388(1)	16(1)
F(7*)	0.566(2)	0.444(1)	0.327(1)	14.5(10)
F(8*)	0.623(1)	0.448(1)	0.4400(8)	7.3(5)

[a] $B_{eq} = (8/3)\pi^2(U_{11}(aa^*)^2 + U_{22}(bb^*)^2 + U_{33}(cc^*)^2 + 2U_{12}aa^*bb^* \cos \gamma) + 2U_{13}aa^*cc^* \cos \beta) + 2U_{23}bb^*cc^* \cos \alpha)$.

Table 5. Selected Bond Distances (Å) and Angles (deg) for $Rh_2(DTolF)_2(O_2CCF_3)_2(CH_3CN)_2$ (**1**)

Rh(1)−Rh(2)	2.474(5)	Rh(1)−N(3)	2.267(5)
Rh(1)−N(1)	2.007(4)	Rh(2)−N(6)	2.011(4)
Rh(1)−N(5)	2.015(4)	Rh(2)−N(2)	2.011(4)
Rh(1)−O(3)	2.094(3)	Rh(2)−O(1)	2.098(3)
Rh(1)−O(2)	2.101(3)	Rh(2)−O(4)	2.100(3)
Rh(2)−N(4)	2.265(5)		
N(1)−Rh(1)-N(5)	91.6(2)	N(1)−Rh(1)-O(3)	87.93(14)
N(5)−Rh(1)-O(3)	175.2(2)	N(1)−Rh(1)-O(2)	175.4(2)
N(5)−Rh(1)-O(2)	88.2(2)	O(3)−Rh(1)-O(2)	91.92(14)
N(1)−Rh(1)-N(3)	97.1(2)	N(5)−Rh(1)-N(3)	101.2(2)
O(3)−Rh(1)-N(3)	83.64(14)	O(2)−Rh(1)-N(3)	87.6(2)
N(6)−Rh(2)-N(2)	91.7(2)	N(6)−Rh(2)-O(1)	174.80(2)
N(2)−Rh(2)-O(1)	88.40(2)	N(6)−Rh(2)-O(4)	88.2(2)
N(2)−Rh(2)-O(4)	175.0(2)	O(1)−Rh(2)-O(4)	91.22(14)
N(6)−Rh(2)-N(4)	93.9(2)	N(2)−Rh(2)-N(4)	99.3(2)
O(1)−Rh(2)-N(4)	91.27(14)	O(4)−Rh(2)-N(4)	85.7(2)
N(2)−C(40)-N(1)	124.4(5)	N(5)−C(39)-N(6)	125.8(5)
O(1)−C(28)-O(3)	129.7(5)	O(2)−C(31)-O(4)	131.4(5)
N(4)−Rh(2)-Rh(1)	172.37(11)	N(3)−Rh(1)-Rh(2)	168.88(11)

Table 6. Selected Bond Distances (Å) and Angles (deg) for $[Rh_2(DTolF)_2(CH_3CN)_6][BF_4]_2$ (**5**)

|			
Rh(1)−Rh(2)	2.5594(8)	Rh(2)−N(2)	2.026(6)
Rh(1)−N(1)	2.042(7)	Rh(2)−N(4)	2.017(2)
Rh(1)−N(5)	2.029(7)	Rh(2)−N(6)	2.018(7)
Rh(1)−N(3)	2.037(6)	Rh(2)−N(10)	2.208(7)
Rh(1)−N(9)	2.235(7)	Rh(2)−N(8)	2.023(2)
Rh(1)−N(7)	2.020(6)		
Rh(1)−N(1)-C(47A)	161.9(26)	Rh(2)−N(2)-C(17)	173.9(8)
C(10)−N(10)-Rh(1)	170.5(6)	C(32)−N(9)-Rh(1)	175.0(9)
N(9)−Rh(1)-N(6)	178.6(3)	N(9)−Rh(1)-N(5)	92.9(4)
N(6)−Rh(1)-N(10)	92.0(2)	N(9)−Rh(1)-N(1)	85.5(3)
N(5)−Rh(1)-N(10)	177.4(3)	N(5)−Rh(1)-N(1)	93.1(3)
N(6)−Rh(1)-N(1)	93.8(2)	N(4)−Rh(2)-N(3)	87.8(10)
N(10)−Rh(1)-N(1)	84.3(2)	N(3)−Rh(2)-N(7)	96.4(4)
N(4)−Rh(2)-N(7)	174.8(14)	N(3)−Rh(2)-N(8)	175.3(16)
N(4)−Rh(2)-N(8)	96.4(3)	N(4)−Rh(2)-N(2)	99.1(13)
N(7)−Rh(2)-N(8)	79.3(9)	N(7)−Rh(2)-N(2)	83.6(2)
N(3)−Rh(2)-N(2)	95.8(11)	N(4)−C(3)-N(5)	125.0(14)
N(3)−C(2)-N(6)	125.2(6)	N(2)−C(17)-C(40)	178.0(12)
N(1)−C(47A)-C(48A)	162.0(58)	Rh(1)−Rh(2)-N(2)	177.8(6)
N(3)−Rh(2)-Rh(1)−N(6)	7.8(6)	Rh(2)−Rh(1)-N(1)	174.9(13)
N(4)−Rh(2)-Rh(1)−N(5)	8.5(5)	N(1)−C(1)-N(2)	123.4(7)
N(7)−C(1)-C(7)−N(8)	2.2(11)		

Table 7. Selected Bond Distances (Å) and Angles (deg) for $[Rh_2(DTolF)_2(9\text{-}EtAH)_2(CH_3CN)][BF_4]_2$ (**6**)

Rh(1)−Rh(2)	2.510(3)	Rh(1)−N(1)	2.04(2)
Rh(1)−N(2)	2.04(2)	Rh(1)−N(3)	2.07(2)
Rh(1)−N(4)	1.99(2)	Rh(1)−N(5)	2.06(2)
Rh(2)−N(6)	2.03(2)	Rh(2)−N(7)	2.00(2)
Rh(2)−N(8)	2.03(2)	Rh(2)−N(9)	2.03(2)
N(1)−Rh(1)-N(2)	177.7(8)	N(1)−Rh(1)-N(3)	92.1(7)
N(1)−Rh(1)-N(4)	88.6(7)	N(1)−Rh(1)-N(5)	98.9(8)
N(2)−Rh(1)-N(3)	87.1(7)	N(2)−Rh(1)-N(4)	92.1(7)
N(2)−Rh(1)-N(5)	83.2(8)	N(3)−Rh(1)-N(4)	176.4(8)
N(3)-Rh(1)-N(5)	90.1(7)	N(4)-Rh(1)-N(5)	93.3(8)
N(6)−Rh(2)-N(7)	89.5(8)	N(6)−Rh(2)-N(8)	91.8(7)
N(6)−Rh(2)-N(9)	179.0(7)	N(7)−Rh(2)-N(8)	176.5(7)
N(7)−Rh(2)-N(9)	89.6(7)	N(8)−Rh(2)-N(9)	89.2(7)
N(1)−C(1)-N(9)	116(2)	N(3)−C(2)-N(7)	118(2)

Figure 3. ORTEP representation of compound **1** drawn at the 50% probability level. H and F atoms are omitted for clarity.
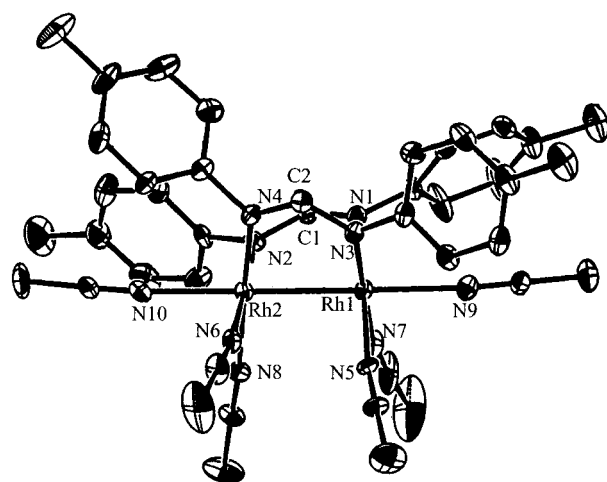
Figure 4. ORTEP representation of compound **5** with thermal ellipsoids drawn at the 50% probability level. H atoms are omitted for clarity.
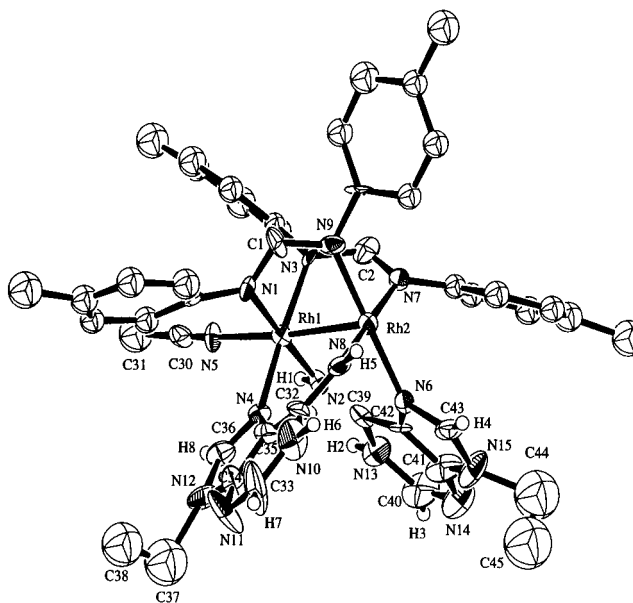
Figure 5. ORTEP representation of compound **6** with thermal ellipsoids drawn at the 50% probability level. H atoms are omitted for clarity.

bridging types of bridging ligands, namely [DTolF]⁻ anions and cis 9-EtAH ligands coordinated in a head-to-tail bridging orientation through the N7 and N6 positions of the purine. This structure constitutes only the second example of a bridging adenine in a metal complex, the first example being $[Mo_2(O_2\text{-}CCHF_2)_2(9\text{-}EtAH)_2(CH_3CN)_2][BF_4]_2$ with the adenine ligand in a head-to-tail arrangement.[4b] The presence of only one axial acetonitrile molecule is unusual, furthermore the Rh−NCCH₃

bond distance of 2.04(2) Å is quite short. Other monoaxial adducts that have recently been prepared in our laboratories, namely $[Rh_2(DTolF)_2(bpy)(CH_3CN)_3][BF_4]_2$, $[Rh_2(DTolF)_2\text{-}(bpy)_2(CH_3CN)][BF_4]_2$, and $[Rh_2(DTolF)_2(phen)(CH_3CN)_3]\text{-}[BF_4]_2$, contain a single axial acetonitrile ligand coordinated at
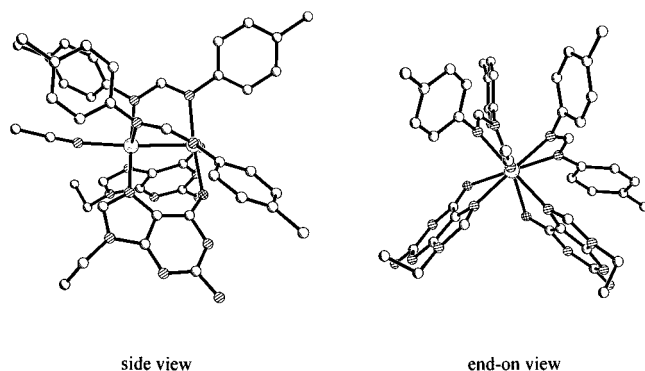
Figure 6. PLUTO representations of compound **7**: (a) side view and (b) end-on view.
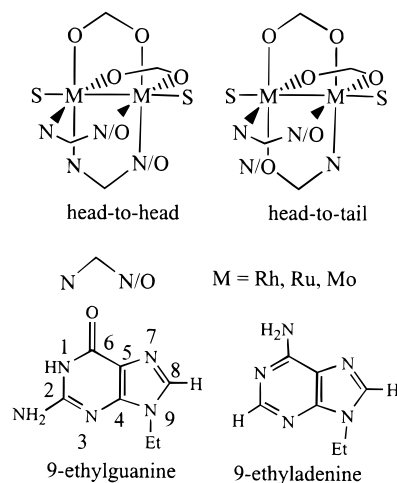
Rh−N bond distances of 2.101(4), 2.115(4), and 2.126(3) Å, respectively.[14] As a consequence of the unsymmetrical structure, the metal−ligand distances to the two purines are slightly different from each other. In one adenine the distances are Rh-(1)−N(4) = 1.99(2) Å and Rh(2)−N(6) = 2.03(2) Å, and in the other adenine the corresponding distances are Rh(1)−N(2) = 2.04(2) Å and Rh(2)−N(8) = 2.03(2) Å. The fact that two outer-sphere [BF$_4$]$^-$ anions are present in the structure allows for the assignment of the 9-EtAH molecules as neutral, but does not resolve the question as to whether the N6 positions are amino (NH$_2$) or imino (NH$^-$) groups. This question will be addressed in the ^{1}H NMR spectroscopy section.

The bridging [DTolF]$^-$ ligands of [Rh$_2$(DTolF)$_2$(9-EtAH)$_2$-(CH$_3$CN)][BF$_4$]$_2$ are twisted from the eclipsed orientation by ∼30°, which is nearly 10° more than the twist exhibited by **5**, and more than 20° greater than that observed for the bis-trifluoroacetate derivatives. The Rh−Rh bond length of 2.510-(3) Å in **6** is slightly shorter than that of the parent complex [Rh$_2$(DTolF)$_2$(CH$_3$CN)$_6$][BF$_4$]$_2$ (**5**), but longer than that observed for Rh$_2$(DTolF)$_2$(O$_2$CCF$_3$)$_2$(CH$_3$CN)$_2$ (**1**). The Mo−Mo bond length in [Mo$_2$(O$_2$CCHF$_2$)$_2$(9-EtAH)$_2$(CH$_3$CN)$_2$][BF$_4$]$_2$ of 2.1436-(17) Å is significantly shorter than the Rh−Rh distance in [Rh$_2$-(DTolF)$_2$(9-EtAH)$_2$(CH$_3$CN)][BF$_4$]$_2$ which indicates that the 9-ethyladenine ligand can span a wide range of dimetal bond distances.

[Rh$_2$(DTolF)$_2$(9-EtGH)$_2$(CH$_3$CN)][BF$_4$]$_2$ (7). Compound **7** crystallizes in the monoclinic space group *P*2$_1$/*n*. The cation consists of a dirhodium cation coordinated to two neutral 9-EtGH groups bridging the dinuclear unit in a head-to-head arrangement, as well as two cis [DTolF]$^-$ ligands, and one axial CH$_3$CN molecule (Figure 7).

The presence of two [BF$_4$]$^-$ anions in the interstices indicates that the guanine ligands are neutral in this compound. Due to the fact that the data for this structure are so poor, no discussion of the distances or angles is included. This information is contained in the Supporting Information.

NMR Spectroscopic Data. Rh$_2$(form)$_2$(9-EtGH)$_2$(O$_2$CCF$_3$)$_2$ (form = DTolF (3) and DPhF (4)). The use of ^{1}H NMR spectroscopy to characterize dinuclear metal centers coordinated to DNA purines is convenient because of the characteristic downfield shift of the H8 resonance by 0.5−1 ppm upon coordination of the N7 position.[17] The ^{1}H NMR spectra of the products Rh$_2$(DTolF)$_2$(9-EtGH)$_2$(O$_2$CCF$_3$)$_2$ (**3**) and Rh$_2$(DPhF)$_2$-(9-EtGH)$_2$(O$_2$CCF$_3$)$_2$ (**4**) in CD$_3$CN each exhibit two signals in a 1:1 ratio (7.99 and 8.02 ppm for **3** and 7.93 and 8.03 ppm for

(17) (a) Burgess, J. *Trans. Met. Chem.* **1993**, *18*, 439. (b) Hollis, L. S.; Amundsen, A. R.; Stern, E. W. *J. Med. Chem.* **1989**, *32*, 136. (c) Allesio, E.; Balducci, G.; Calligaris, M.; Costa, G.; Attia, W. M.; Mestroni, G. *Inorg. Chem.* **1991**, *30*, 609.

Figure 7. Schematic representations of the H−H and H−T bridging modes of 9-EtGH and 9-EtAH with dinuclear transition metal centers.
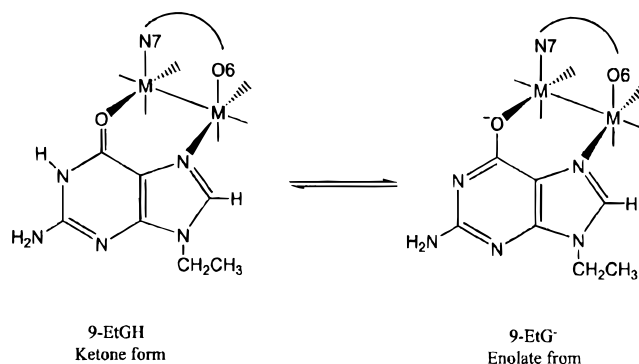
Figure 8. Schematic representations of protonated and deprotonated 9-ethylguanine ligands.

4) attributable to the H8 positions of bridging 9-EtGH molecules. The fact that two resonances are observed is an indication that two isomers are present, namely the head-to-head and head-to-tail isomers depicted in Figure 7. These form in statistical ratios due to the fact that there is no strong preference for formation of the nonpolar versus the polar arrangement of the two purines. These results are in accord with earlier observations that reactions of Rh$_2$(O$_2$CCH$_3$)$_4$ and [Rh$_2$(O$_2$CCH$_3$)$_2$(CH$_3$CN)$_6$]$^{2+}$ with 9-EtGH lead to both isomers as verified by X-ray crystallography.[4]

Earlier work in our laboratories had established that reactions of Rh$_2$(O$_2$CCH$_3$)$_4$L$_2$, [Rh$_2$(O$_2$CCH$_3$)$_2$(CH$_3$CN)$_6$][BF$_4$]$_2$, and Rh$_2$(O$_2$CCF$_3$)$_4$ with 9-ethylguanine lead to products with one of two types of bridging guanine ligands. These are 9-EtGH, the neutral ligand form and 9-EtG$^-$, the anionic or deprotonated form (Figure 8). It has been documented that the pK_a of the N1 position is lowered by 1.5−2.0 pK_a units upon coordination to platinum complexes (from ∼9.4 to 8.0).[18] The deprotonation of the N1−H in guanine to give 9-EtG$^-$ has been observed mainly in reactions with metal complexes containing basic leaving groups such as CH$_3$CO$_2^-$ (pK_b = 9.25). The much lower basicity of the CF$_3$CO$_2^-$ leaving group (pK_b > 13) results exclusively in the formation of products containing the neutral 9-EtGH form. It therefore is reasonable to expect that a leaving group such as CH$_3$CN would lead only to compounds with neutral guanine ligands.

The ^{19}F NMR spectra of compounds **3** ($\delta = -12.49$) and **4** ($\delta = -12.47$ ppm) are indicative of dissociated [CF$_3$CO$_2$]$^-$ groups in solution (Table 9).[19] This conclusion is based on ^{19}F NMR signals for bridging, equatorial [CF$_3$CO$_2$]$^-$ groups which

Table 8. ^{1}H NMR Spectroscopic Data for
[Rh$_2$(DTolF)$_2$(9-EtAH)$_2$(CH$_3$CN)][BF$_4$]$_2$ (**6**)

solvent	T (°C)	H1	H2	H8	H6	N−CH−N
CD$_3$CN	25		7.68	8.06		7.26
CD$_3$CN	−32		7.68	8.04	6.46	7.65
acetone-d_6	25		7.94	8.63	11.35	7.73
acetone-d_6	−41	7.20	7.99(d)	8.73	11.57	7.71

Table 9. ^{19}F NMR Spectroscopic Data for **3** and **4** (Measured in
CD$_3$CN and Acetone-d_6 at 25 °C, Referenced to C$_6$H$_5$CF$_3$)

	chemical shift assignments, ppm
3, Rh$_2$(DTolF)$_2$(9-EtGH)$_2$(O2CCF$_3$)$_2$	−12.49 (s, O$_2$CCF$_3$)
4, Rh$_2$(DPhF)$_2$(9-EtGH)$_2$(O$_2$CCF$_3$)$_2$	−12.47 (s, O$_2$CCF$_3$)

are commonly observed 50−60 ppm upfield ($\delta \sim -77$ ppm)
from the free acid referenced to C$_6$H$_5$CF$_3$. Monodentate, axially
coordinated [CF$_3$CO$_2$]$^-$ ligands have been observed in the same
chemical shift region as the uncoordinated ligand.[19]

[Rh$_2$(DTolF)$_2$(CH$_3$CN)$_6$][BF$_4$]$_2$ (5). The ^{1}H NMR spectrum
of [Rh$_2$(DTolF)$_2$(CH$_3$CN)$_6$][BF$_4$]$_2$ (**5**) is in accord with the solid-
state structure obtained from the crystallographic results. The
singlet at $\delta = 1.96$ ppm is assignable to free acetonitrile ligands
that have undergone exchange with CD$_3$CN, whereas the singlet
at $\delta = 2.49$ ppm can be attributed to equatorial acetonitrile
groups. The singlet at $\delta = 2.27$ ppm is due to the four equivalent
methyl groups of the tolyl substituents on the formamidinate,
and a multiplet centered at $\delta \sim 6.9$ ppm is assigned to the phenyl
rings. The triplet centered at $\delta = 7.51$ ppm is observed for the
H atom of the N−CH−N fragment of the formamidinate groups
with [103]Rh−[1]H coupling of 30 Hz.

[Rh$_2$(DTolF)$_2$(9-EtAH)$_2$(CH$_3$CN)][BF$_4$]$_2$ (6). The ^{1}H NMR
data for [Rh$_2$(DTolF)$_2$(9-EtAH)$_2$(CH$_3$CN)][BF$_4$]$_2$ (**6**) proved to
be quite useful in resolving the question as to whether the N6
positions of the purines were amino (NH$_2$) or imino (NH$^-$)
groups. The latter situation, although unusual, arises from a
prototopic shift from the N6 amino group to the N1 position of
the purine (Figure 9). For example, a prototopically shifted
adenine is present in the compound [Mo$_2$(O$_2$CCHF$_2$)$_2$(9-EtAH)$_2$-
(CH$_3$CN)$_2$][BF$_4$]$_2$.[4b] A prototopic shift in 9-EtAH is easily
recognized by ^{1}H NMR spectroscopy, since three resonances
are expected for the common adenine tautomer, whereas four
resonances are expected for an adenine that had undergone a
prototopic shift from N6 to N1. The ^{1}H NMR spectrum of **6** in
CD$_3$CN exhibits two singlets that can be assigned to the H8
(8.06 ppm) and H2 (7.68 ppm) protons in the aromatic region
(Table 8, Figure 10). Upon lowering the temperature to −32
°C, an additional singlet appears at 6.46 ppm that can be
assigned to the NH6 protons. The observation of these three
resonances initially led us to conclude that the 9-EtAH ligands
were neutral with the two protons of the exocyclic NH$_2$ group
intact. By measuring the ^{1}H NMR spectrum in acetone-d_6,
however, we were led to a different conclusion. The room
temperature ^{1}H NMR spectrum in acetone-d_6 exhibits singlets
at 7.94, 8.63, and 11.35 ppm that are assignable to the H2, H8,
and H6 protons, respectively, but at −41 °C the resonance at
7.94 is resolved into a doublet, and a new resonance appears at
7.20 ppm (H1) among the aromatic resonances of the [DTolF]$^-$
groups. The integration of the four resonances is 1:1:1:1, with
the definitive assignments of the H1 and H2 protons being

confirmed by selective decoupling experiments. The solution
behavior in acetone allows for the definitive assignment of the
adenine structure and supports the X-ray results for **6**.

[Rh$_2$(DTolF)$_2$(9-EtGH)$_2$(CH$_3$CN)][BF$_4$]$_2$ (7). The bulk prod-
uct obtained from the reaction of [Rh$_2$(DTolF)$_2$(CH$_3$CN)$_6$][BF$_4$]$_2$
(**5**) with 2 equiv of 9-EtGH exhibits two H8 resonances in a
1:1 ratio in CD$_3$OD at $\delta = 8.32$ and 8.35 ppm. The two triplets
observed for the N−CH−N signals at $\delta = 7.50$ and 7.55 ppm
are an indication of two types of formamidinate environments
and further reveal coupling to the rhodium nuclei [3]J([103]Rh−
[1]H) coupling of 30 Hz. The broad resonances in the aromatic
region of the formamidinate ligand as well as the broadened
ethyl regions of the purine ligands point to a mixture of
compounds. A ^{1}H NMR spectrum obtained from crystals of
[Rh$_2$(DTolF)$_2$(9-EtGH)$_2$(CH$_3$CN)][BF$_4$]$_2$ (**7**) with the head-to-
head arrangement exhibited one H8 signal at 8.34 ppm which
indicated that selective crystallization of this isomer had been
effected. Attempts to isolate the pure head-to-tail isomer have
not been successful.

Electrochemistry of 5, 6, and 7. The cyclic voltammogram
of [Rh$_2$(DTolF)$_2$(CH$_3$CN)$_6$][BF$_4$]$_2$ (**5**) exhibits one reversible
oxidation at $E_{1/2} = +1.02$ V and one quasi-reversible oxidation
at $E_{p,a} = +1.55$ V with an associated return wave at $E_{p,c} =
+1.40$ V. Two irreversible reductions are located at $E_{p,c} = -0.51$
and −1.34 V in comparison to the bis-trifluoroacetate adduct,
which exhibits only two reversible metal-based oxidations at
$E_{1/2} = +0.52$ and +1.41 V, and an irreversible oxidation at
+0.95 V attributed to free formamidinate.[7b] Replacement of
equatorial acetonitrile ligands with 9-EtGH affects the electronic
properties of the dirhodium core as clearly indicated by the
electrochemistry of [Rh$_2$(DTolF)$_2$(9-EtGH)$_2$(CH$_3$CN)][BF$_4$]$_2$,
(**6**). This compound exhibits a reversible oxidation at $E_{1/2} =
+0.67$ V, a quasi-reversible oxidation at $E_{1/2} = +1.63$ V and
an irreversible reduction at −1.31 V. An even more dramatic
change in the electrochemical properties is observed when the
bridging purines are 9-EtAH. [Rh$_2$(DTolF)$_2$(9-EtAH)$_2$(CH$_3$CN)]-
[BF$_4$]$_2$ (**7**) exhibits one irreversible anodic process at $E_{p,a} =
+0.93$ V with a very small return wave at +0.72 V. An
irreversible reduction process near the solvent limit is observed
at $E_{p,c} = -1.14$ V.

The electrochemical behavior of the dirhodium compounds
is clearly influenced by the identity of the ligands trans to the
formamidinate ligands. It appears that the most stable dirhodium-
(II,II) compound in the group we examined is [Rh$_2$(DTolF)$_2$-
(9-EtAH)$_2$(CH$_3$CN)][BF$_4$]$_2$ in that it is more difficult to oxidize
or reduce than either [Rh$_2$(DTolF)$_2$(9-EtGH)$_2$(CH$_3$CN)][BF$_4$]$_2$
or [Rh$_2$(DTolF)$_2$(CH$_3$CN)$_6$][BF$_4$]$_2$. This may be an important
factor in determining the most stable adducts of the antitumor
active dirhodium compounds with DNA.

Conclusions

Recent findings in our laboratories involving the reactions
of dirhodium tetracarboxylate compounds with DNA purines
raises the question of the possible involvement of the O6/N6
positions of guanine and adenine in the DNA binding of this
class of compounds. Reactions of Rh$_2$(form)$_2$(O$_2$CCF$_3$)$_2$(CH$_3$-
CN)$_2$ and [Rh$_2$(DTolF)$_2$(CH$_3$CN)$_6$][BF$_4$]$_2$ with purines were
explored, and it was found that the 9-ethylguanine ligands adopt
bridging arrangements, with no apparent preference for either
head-to-head or head-to-tail isomers. On the other hand,
reactions of [Rh$_2$(DTolF)$_2$(CH$_3$CN)$_6$]$^{2+}$ with 9-EtAH yield only
the head-to-tail isomer. ^{1}H NMR studies support the conclusion
that the adenine has undergone a prototopic shift of an NH$_2$
proton to the N1 position, a situation that reflects the change

(18) Lippard, S. J. *Pure Appl. Chem.* **1987**, *59*, 731.
(19) (a) Webb, G. A. *Annu. Rep. NMR Spectrosc.* **1983**, 14. (b) Garner, C.
D.; Hughes, B. *Adv. Inorg. Radiochem.* **1975**, *17*, 1. (c) Matonic J.
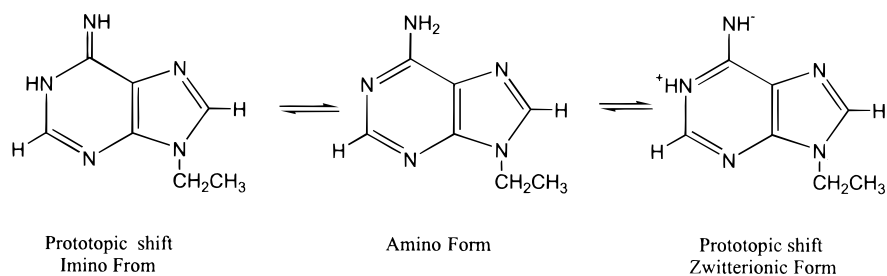H.; Chen, S. J.; Pence, L. E.; Dunbar, K. R. *Polyhedron* **1992**, *11*,
541.

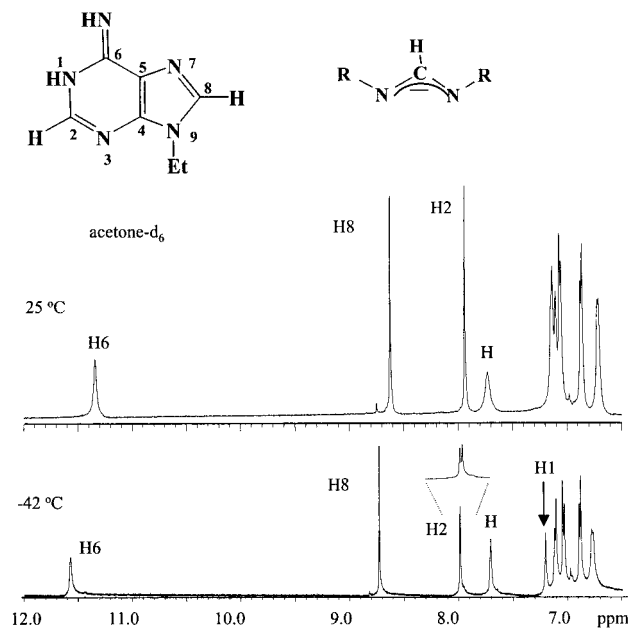**Figure 9.** Schematic representations of 9-ethyladenine tautomers.

Figure 10. ^1H NMR spectra of $[Rh_2(DTolF)_2(9\text{-}EtGH)_2(CH_3CN)][BF_4]_2$ (**6**).

in acidity of these protons upon coordination of the N7 position to the metal. It is clear from these new studies that dirhodium formamidinate reactions with DNA nucleobases proceed in a manner that is very similar to the corresponding reactions of dirhodium tetracarboxylate compounds. An obvious extrapolation of these and earlier results from our laboratories is an exploration of the more biologically relevant reactions of dimetal complexes with single- and double-stranded DNA. Preliminary work involving dirhodium acetate reactions in water with dinucleotides as well as dodecamer -GpG- and -ApA- containing sequences of DNA points to the formation of a single product. Attempts to elucidate the structures of these products by two-dimensional NMR methods as well as X-ray crystallography are in progress and will be reported in due course.[20]

Supporting Information Available: Tables of crystal data and listings of atomic coordinates, bond lengths and bond angles, anisotropic thermal parameters, and torsion angles for **1**, **5**, **6**, and **7**. This material is available free of charge via the Internet at http://pubs.acs.org.

IC990194N

(20) Lozada, E.; Catalan, K. V.; Chifotides, H.; Sorasaenee, K.; Bishop, K.; Dunbar, K. R. Unpublished results.